INTERNATIONAL JOURNAL OF
COASTAL & OFFSHORE ENGINEERING
IJCOE Vol.4/No. 1/Spring 2020 (1-9)

Available online at: www. Ijcoe.org

The choice between Radial Basis function and Feed Forward Neural Network to predict long term tidal condition

Hengameh Motamedi[1], Maryam Rahbani [2]*, Abbas Harifi[3], Danial Ghaderi[4]

[1] *MSc. Student, Faculty of Marine Science and Technology, University of Hormozgan, Bandar Abbas 79131, Iran; hengameh.motamedi@gmail.com*
[2*] *Associate Professor, Faculty of Marine Science and Technology, University of Hormozgan, Bandar Abbas 79131, Iran; maryamrahbani@yahoo.com*
[3] *Assistant Professor, Department of Electrical and Computer Engineering, University of Hormozgan, Bandar Abbas 79131, Iran; harifi@hormozgan.ac.ir*
Ph.D. Student, Faculty of Marine Science and Technology, University of Hormozgan, Bandar Abbas 79131, Iran; danialghaderi1@gmail.com

ARTICLE INFO

Article History:
Received: 02 Sep. 2020
Accepted: 18 Oct. 2020

Keywords:
Feed Forward Neural Network
Radial Basis Functions
Tidal Prediction
Beris port

ABSTRACT

Possessing precise water level data in any coastal area is crucial, for any coastal engineering or managements. One of the main processes responsible for a regular water level changes is tide. Due to its nature, tidal prediction is relatively easily accessible. However, the precision of the results depends on the number of constituents have been considered for the prediction. The aim of this paper is to identify the most relevant tidal constituents and their relevant amplitudes for tidal prediction in the Beris port, south of Iran, using artificial neural network (ANN). The main constituents in the area is obtained as M_2, K_1, S_2, N_2 and O_1. To regenerate the tidal condition considering these constituents two ANN methods has been applied including Feed Forward, and Radial Basis Functions (RBF). For the training and network test tidal data of the year 2017 has been considered. For the training a variety of months and constructions has been applied. For the Feed-Forward the Levenberg-Marquardt learning method has been considered. After executing different structures in terms of the number of neurons in the hidden layer and taking into account the minimum error and run time, the network with 5 neurons in the hidden layer and two months training was qualified. For the RBF, the radius of 2.5 has been qualified. The evaluated network of both Feed-Forward and RBF has been employed to reproduce tidal water level of the whole year 2018, and the results were compared with both field data and those derived from harmonic analysis. It was found that the three layers Feed-Forward network shows the best performance in tidal prediction with the correlation coefficient of 0.85, which is followed by RBF, with the correlation coefficient of 0.81.

1. Introduction

Sea level fluctuations caused by celestial gravitational forces and Earth's rotation is known as the tide. The effect of either of the celestial motions or forces including the sun and the moon is introduced as a tidal constituent [1–3]. Thus, each constituent has a specific period, oscillation amplitude, and phase, in which the period is constant throughout the Earth, but the amplitude and phase of each constituent depend on the location of interest [4]. In every aspect of marine science including maritime transport, sedimentation and coastline management, coastal protection, and tidal energy potential assessment, detailed tidal information is required [5, 6]. Table 1 shows the period of fundamental tidal constituents. Each of the frequencies of ω_s, ω_L, ω_1 and ω_5 of Table 1 is used to generate a specific tensile constituent [7, 8].

Table 1: The fundamental astronomical period of motions of the earth, moon and sun [8]

Description	Frequency notation (1/period)	Period (mean solar units)
Sidereal day(one rotation wrt vernal equinox)	Ω	23.9344 hours
Mean solar day(one rotation wrt to the sun)	w_s	24.0000 hours
Mean lonar day(one rotation wrt to the moon)	w_L	24.8412 hours
Period of lunar declination (tropical month)	w_1	27.3216 days
Period of solar declination(tropical year)	w_2	365.2422 days
Period of lunar perigee	w_3	8.847 years
Period of lunar node	w_4	18.613 years
Period of perihelion	w_5	20.940 years

As tides enter the coastal area and shallow water, nonlinear terms of the governing equations on the tidal propagation are activated. These terms represent the effect of shallow water disturbances mathematically, which depending on the type, are divided into two categories including over tide and compound tide [9]. There are several ways to obtain tidal constituents, but the limitations of the areas where an installed buoy records tidal data constantly can sometimes make the acquisition of data difficult and costly. Therefore, tensile prediction methods are always used in terms of time and cost savings. These methods have been developed according to specific region information and do not provide accurate results everywhere. Much research has been done in this field; Lee employed the application of a back-propagation neural network with the short-term measuring data of tidal level in Taichung Harbor in Taiwan to predict the long-term tidal levels [10]. Lee et. al. proposed a program based on harmonic analysis and back-propagation, artificial neural networks to predict tidal condition using short-term measurement data of sea-level records from the Hillarys Boat Harbor tide gauge, Western Australia. The results show that short-term sea-level registrations can be efficiently employed to produce accurate tidal predictions [11]. Okwuashi and Olayinka used the Kalman filter (KF) to forecast the height of tide based on seven main tidal constituents M_2, S_2, N_2, K_2, K_1, O_1, and P_1. The KF was found to outperform the conventional least squares regression technique [12]. Okwuashi et al. examined the novel use of the partial least squares regression (PLSR) as an alternative model to the conventional least squares (LS) model for modeling tide levels. their model is based on twenty tidal constituents: M_2, S_2, N_2, K_1, O_1, MO_3, MK_3, MN_4, M_4, SN_4, MS_4, $2MN_6$, M_6, $2MS_6$, S_4, SK_3, $2MK_5$, $2SM_6$, $3MK_7$, and M_8 [13].

In this study, the prediction of the tide in the Beris port has been performed by comparing two structures of radial basis function (RBF) neural network and three layers feed-forward back-propagation (FFBP) neural network, to find out which one could provide more reliable results. Besides the results are also compared with the harmonic analysis method.

2. Materials and Methods

2.1. Tidal prediction with harmonic analysis

The most common method to analyze tide is harmonic analysis. According to the theory, tidal analysis is the process of breaking a specific tide into its basic constituents. It means considering the effect of the moon, the sun, and their combined effect separately, as well as the shape of the coast and seabed topography [14].

The general equation of harmonic analysis is presented below. Total number of significant tidal constituents are selected considering the duration of tidal oscillation. Therefore, The height of the tide at time *t* can be computed by expressing it as the sum of harmonic terms [13];

$$Y(t) = A_0 + \sum_{i=1}^{N} h_i \cos(\omega_i t + \varepsilon_i) \quad (1)$$

For accurate tidal analysis, all astronomical periods must be used, meaning 18.6 years of sea-level observations are needed, which is quite a time consuming and in most of the coastal area is still not available. This issue can be resolved by entering the related components of the moon, the sun, and other parameters involved, in the equations and calculating the effects of these constituents. The linear model of the above equation is in the form of Equation 2.

$$h(t) = A_0 + \sum_{i=1}^{N} (A_i \cos(\omega_i t) + B_i \sin(\omega_i t)) \quad (2)$$

where, A_0 is the height of mean water level above the datum, A_i and B_i are the tidal constituent amplitudes, ω_i represents the tidal frequencies, *h(t)* denotes the height of the tide at time *t*, and *N* is the number of tidal constituents selected for tidal analysis [13], [15]. Having instantaneous water level records in a location, tidal constituent amplitudes can be calculated, for tidal prediction.

2.2. Artificial neural networks

Artificial neural networks (ANN) is a subset of artificial intelligence techniques, it's structure and function of which are like those of the human brain [16]. This system is consists of a large number of processing elements called neurons that coordinate with each other to solve a problem and connect input to output [17]. A neural network includes layers and weights, and its behavior dependents on the relationship between members. A neural network is composed of input, hidden and output layers. The input layer only receives the information and acts as an independent variable; on the other hand, the outer layer functions as the dependent variable and the number of its neurons depends on the number of dependent variables. In addition to the input and output layers, a neural network also includes a hidden layer which is the main part of processing [18].

A neural network is made up of artificial neurons which has the task of data processing. These neurons are connected to each other, to process received input information, and produce the desired output through the appropriate transfer function. The actual output depends on the special transfer function selected.

There are different types of ANN with different transfer functions, each with its own capabilities and features, so a suitable neural network must be selected to achieve the desired prediction result. In this study, a multilayer feed-forward neural network, as a well-known method, has been compared with the radial functions neural network for tidal prediction, in order to find which one is more reliable for tidal prediction.

2.2.1. Feed Forward Back-Propagation (FFBP) Neural Network

The most common back-propagation neural network architecture is the multilayer FFBP [19–21]. In this method network processors are divided into several layers, the minimum number of layers in these networks being two. Figure 1 shows the structure of a two (Figure 1A) and three (Figure 1B) layers FFBP network.

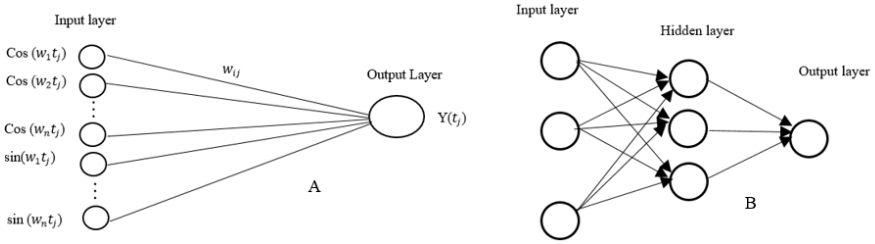

Figure 1: Structure of FFBP Network. A) Two layers and B) Three layers [14]

As mentioned, appropriate transfer functions must be selected according to the type of function and layer used. In the three-layer FFBP network, the tan-sigmoid transfer function and linear transfer function are used [22, 23]. Relationships 3 show how to obtain the tan-sigmoid functions: [24].

$$F(x) = \frac{1}{(1 + e^{-1})} \qquad (3)$$

An important aspect of the ANN is their training process. Training is generally a process that determines the weight and bias. There are different training algorithms to train the neural network, Levenberg-Marquardt among them is the one used in this study. The Levenberg-Marquardt is a method in which the second derivative known as the Hessian matrix is used in addition to the first derivative (the Jacobian matrix). One of the advantages of this method is that it does not need to determine the learning rate from the beginning and the algorithm is able to adjust the learning rate adaptively [25, 26]. In this algorithm, the method of changing the processing parameters of neural network neurons is calculated from relationship 4:

$$X_{k+1} = xk - [H + \eta^I]^{-1}\ J^T\ e(t) \qquad (4)$$

Where, *k* is repetitive learning counter, *x* represents the vector of weights and bias, *e(t)* denotes the error, is the training rate, *H* represents the Hessian matrix, and *J* represents the Jacobson matrix [27].

2.2.2. Radial Basis Function (RBF) Neural Network

The network of RBF requires a large number of neurons for training. The performance of these networks is also best achieved if a large number of training vectors are used [28]. RBF networks have just two layers (Figure 2), the first of which is of radial basis type and the output layer is linear. The network parameters here include the spread number and the goal number. By changing these two parameters, the network performance can be improved [29, 30].

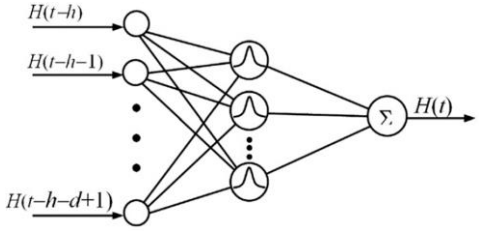

Figure 2: Structure of Radial Basis Function Neural Network [31]

The Gaussian transfer function is used in the RBF network [8]. Relationship 5 show how to obtain Gaussian transfer functions:

$$F(x) = a\, e^{-\frac{(x-b)^2}{2c2}} \quad (5)$$

where, *e* is Euler's number, *a*, *b* and *c* are real constant coefficients.

2.3. Study Area

For this study Beris port has been chose, which is located along the Makran coasts, northern part of the Gulf of Oman. This port has been selected since it has a characteristic of a coastal ocean. Longitude and latitude of the Beris port is 61°10´ and 25°08´ respectively. This port is located 85 km east of Chabahar [32, 33]. The water depth inside the por is approximately 5 meters [34]. The port of Beris bordered from the east by Goiter Bay and from the west by the Chabahar Bay. The port of Beris is mostly known as fishing port [32]. The average temperature is 36.2 °C in summer and 16 °C in winter. According to the tidal records, the highest and the lowest tidal range in this port is about 2.97m, and 1 m respectively. In addition, tidal regime in the port is semidiurnal type. Figure 3 shows the location of the Makran coast and the Beris port. As it can be seen Gulf of Oman is the extension of Indian ocean; Thus, the water depth in the coastal area deepen suddenly. Figure 3 shows the bathymetry of the area according to the ETOP1 data [35], and Figure 3B specifically shows that the depth around the Beris port is about 20 to 30 m.

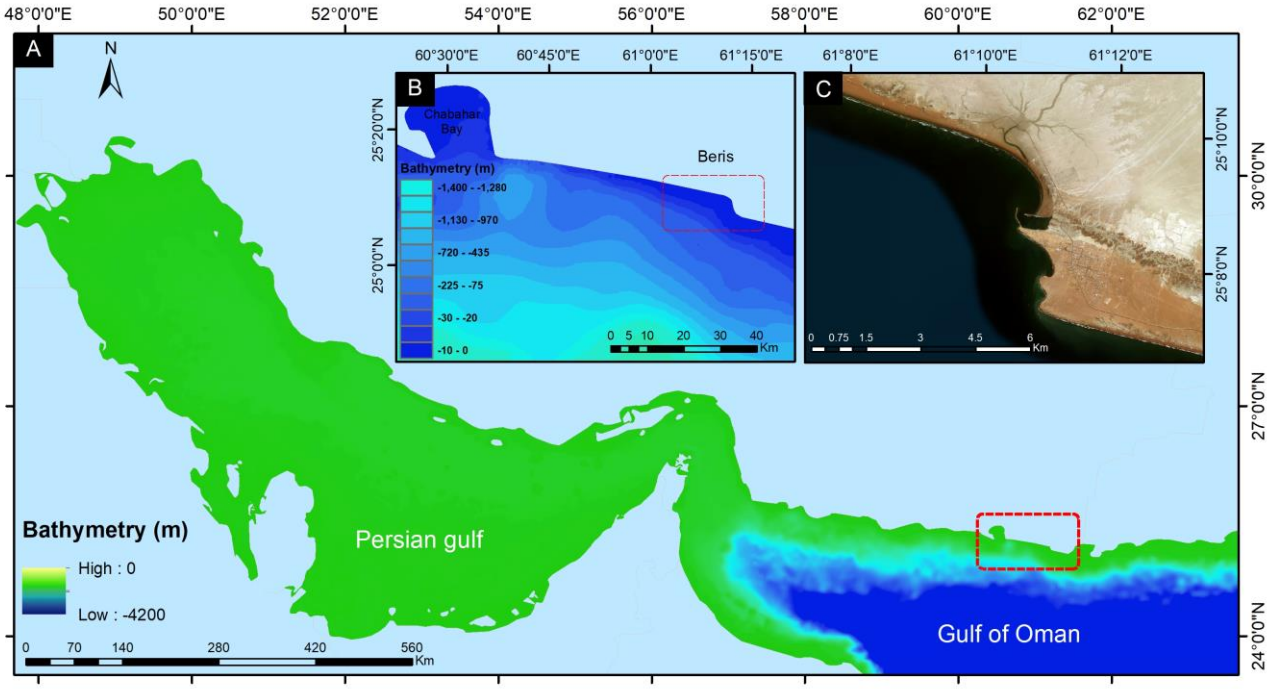

Figure 3: Location of the Beris port, relative to Iran and the Gulf of Oman. A) Bathymetry of the Persian Gulf and the Gulf of Oman, B) Bathymetry changes in areas near Beris port (Taken from ETOPO1 data [35]), and C) Satellite image of Beris port (Taken from Landsat 8 RGB bands) [36]

2.4. The evaluation method

To evaluate the accuracy of the proposed method, the mean squared error (MSE) index and correlation coefficient (R) are used. Relationships 6 and 7 show how these indices are obtained.

$$MSE = \frac{\sum_i^N (y_i - x_i)^2}{N} \quad (6)$$

$$R = \frac{\sum (x_i - \bar{x})\,(y_i - \bar{y})}{\sqrt{\sum (x_i - \bar{x})^2 \;\; \sum (y_i - \bar{y})^2}} \quad (7)$$

In relationships 6 and 7, x_i is the measured data, y_i is the predicted data, N is the number of data, $\bar{x}$ is the mean of the measured data, and $\bar{y}$ is the mean of the predicted data.

3. Results and discussions

3.1. Determining suitable tidal constituent for neural network inputs

It is obvious that considering the more number of tidal constituents means the closer condition to the reality. However, it should be considered that adding too many tidal constituents in ANN does not necessarily improve the predictive results. Sometimes adding unnecessary constituents only slightly improves results, and sometimes confuses the learning process. Therefore, at the very beginning the main tidal constituents efficient,

in the area under investigation, must be determined. That is, to apply major tidal constituents and their corresponding weights as input to the ANN. For this, the neural network structure without a hidden layer (Figure 1A) has been used. Lee, Lee at al. and Anran et. al. showed that 42 tidal constituents as input to ANN will cause optimal performance, for predicting tidal oscillation [10, 11], [37]. The tidal data of the years 2017 and 2018 has been used for network training and network testing respectively. To find out the proper months of training, the method of trial and error has been considered. Table 2 shows part of the procedure. Between 2 and 5 months of training, as the months of training increases, the order of tidal constituents involved, and their amplitude change. Above 5 training months, the ten most important tidal constituents are constant, and their corresponding amplitude varies slightly. Thus, 5 training months were considered.

Table 2: Trial to find proper number of training months

Training Months	Ten most important constituents	Corresponding Amplitude	MSE	Correlation coefficient
2	M_1, No_1,CHI_1 ,S_2,BET_1 ,R_2,M_2,T_2, SA,S_1	5.31, 4.77, 1.05, 1.02, 0.70, 0.67, 0.46, 0.44, 0.36, 0.37	60.78	0.04
3	M_2,S_2,K_1, M_1, N_2 , No_1,O_1,R_2,T_2,S_1	0.46, 0.26, 0.21, 0.17, 0.17, 0.16, 0.12, 0.08, 0.06, 0.05	0.19	0.75
4	M_2,S_2,K_1,N_2,O_1, No_1, M_1, S_1, R_2, NU_2	0.45, 0.21, 0.21, 0.15, 0.12, 0.063, 0.061, 0.060, 0.057, 0.045	0.15	0.78
5	***M_2, K_1, S_2, N_2, O_1, S_1, NU_2, MSF, P_1, No_1***	***0.44, 0.20, 0.19, 0.14, 0.11, 0.046, 0.044, 0.041, 0.035,0.032***	***0.13***	***0.81***
6	M_2, K_1, S_2, N_2, O_1, S_1, NU_2, MSF, P_1, No_1	0.44, 0.21, 0.18, 0.13, 0.11, 0.044, 0.041, 0.041, 0.030, 0.027	0.12	0.83
7	M_2, K_1, S_2, N_2, O_1, S_1, NU_2, MSF, P_1, No_1	0.44, 0.21, 0.18, 0.12, 0.11, 0.04, 0.039, 0.038, 0.028 0.027	0.10	0.84
8	M_2, K_1, S_2, N_2, O_1, S_1, NU_2, MSF, P_1, No_1	0.44, 0.21, 0.18, 0.18, 0.11, 0.040, 0.035, 0.032, 0.029, 0.024	0.10	0.85

The 42 tidal constituents and their corresponding's amplitude derived from the network are presented in Figure 4A, and in descended order in Figure 4B. The major constituents determining the tide at Beris port are the semi-diurnals (M_2, S_2 and N_2) and diurnal (O_1 and K_1) constituents. Among weakly tidal constituents, MS_4 and MN_4 are weaker, so, it seems they do not play important role in this area. Constituent impact ratio implies that the shallow water constituents (M_4 . M_6) are not significant in this area either, which is reasonable considering the feature of the area, with relatively steep coastal slope (Figure 3B).

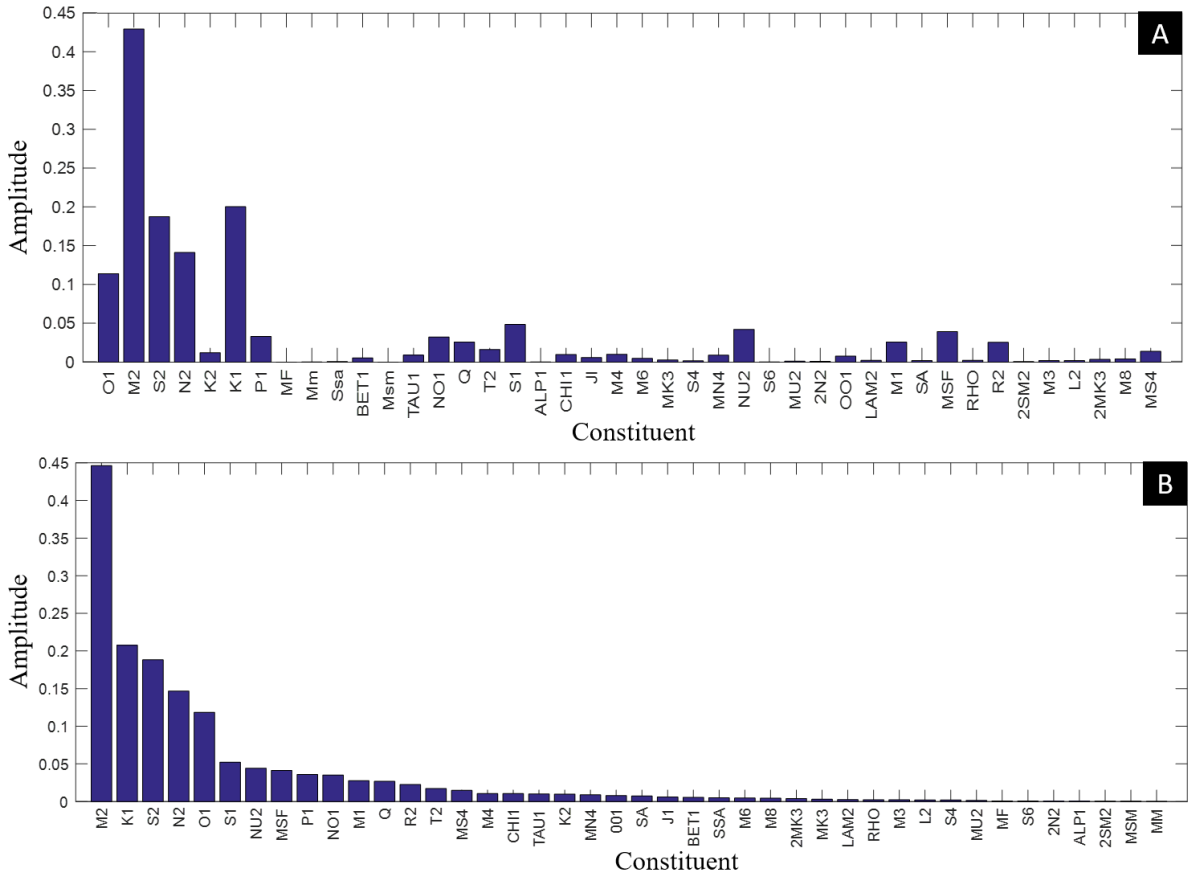

Figure 4: A) The amplitude of 42 tidal constituents shape the tide in Beris port employing 5 months training. B) The same constituents in descending order

Having major harmonic tidal constituents of the area including M_2, K_1, S_2 and O_1, it is possible to calculate Dietrich form number, to determine the regional tidal type [38, 39] for the area under investigation. Employing equation 8 the value of form factor is calculated as 0.49. This means the area can be considered as mixed mainly semidiurnal (0.25 <F <1.5), which is in agreement with Mahmodaf and Bagheri, 2018 study [40].

$$F = \frac{H_{K_1} + H_{o_1}}{H_{M_2} + H_{s_2}} \quad (8)$$

When most relevant tidal constituents and their amplitude verified, these constituents should be used for predicting tidal range of the year 2018. The question is how many of the constituents should be involved to derive precise prediction. To find out the proper number of constituents involved several executions carried out, starting from 4 most relevant constituents. The output results were compared with actual tidal data of 2018, and MSE was calculated. Results are presented in Table 3. It can be seen that the five constituents show the lowest MSE error. Considering Figure 4 it is obvious that the M_2 (the lunar semi-diurnal constituent) has the highest impact, besides, K_1 (Solar and Lunar diurnal constituent), S_2 (the Solar Semi-diurnal constituent), N_2 (Lunar Elliptic Semi-diurnal constituent) and O_1 (Lunar diurnal constituent) have relatively high impact (amplitude). These five constituents therefore selected as inputs for the further procedure.

Table 3: Test of various tidal constituents using FFBP network without the hidden layer (Beris port)

Name of input tidal constituent	MSE
M_2, ,K_1,S_2, N_2	0.1176
M_2, ,K_1,S_2, N_2,O_1	0.1132
M_2, ,K_1,S_2, N_2,O_1, S_1	0.1228
M_2, ,K_1,S_2, N_2,O_1, S_1, NU_2	0.1321
M_2, ,K_1,S_2, N_2,O_1, S_1, NU_2, MSF	0.1412
M_2, ,K_1,S_2, N_2,O_1, S_1, NU_2, MSF, P_1	3.1024
M_2, ,K_1,S_2, N_2,O_1, S_1, NU_2, MSF, P_1, NO_1	21.5272

3.2. Tidal prediction with three-layer FFBP neural network

After the optimum number of tidal constituents were selected, they should be feed to the selected network to be trained for prediction tidal conditions. As mentioned FFBP network is one of the most known among ANN. It has been, therefore, employed for predicting Beris port tidal conditions.

Three layers network was considered proper. Values of $cos(w_i t)$ and $sin(w_i t)$ of the five selected constituents are considered as input layer. A single hidden layer was considered suitable for an overall reliable estimate, which was also suggested by Hornik's, 1989 [41]. Finally, the water level as a tidal condition was considered as output.

Network training was evaluated through bunch of tests with a variety of a number of neurons and days of the year 2017, in order to predict the whole tidal condition of the year 2018. Many tests were performed with 7, 15, 30, and 60 days and 1, 5, 7, 10, and 15 neurons. The output of these tests was compared with the actual field data, and the MSE error and correlation coefficient of them were calculated. The results of some of these tests are presented in Table 4. Among the various tests as shown in Table 4, the lowest error and best correlation belonged to the test with 60 days of observational data and 5 neurons in the hidden layer.

Table 4: Test of various number of hidden layer neurons with the number of days of training (7, 15, 30, 60)

Number of training days	Number of neurons	MSE	Correlation coefficient
7	1	0.14	0.80
7	10	0.15	0.79
15	5	0.13	0.81
15	15	0.12	0.82
30	5	0.12	0.83
30	7	0.13	0.81
60	***5***	***0.10***	***0.85***
60	15	0.12	0.84

3.3. Tidal prediction with Radial Basis Function neural networks

As mentioned before, in RBF network the training can be achieved either when the error reaches the specified limit or when the network reaches the specified number of neurons and stops [42]. Here different radius numbers have been given to the network for the specified error, which has been gained in the three-layer FFBP network. The optimal point is then considered based on the computation time and the number of neurons. The output of each execution was compared with the actual tide data, and MSE error was calculated.

Table 5 represents the radius, number of neurons, and the MSE values for some of the executed tests. As mentioned, the goal for all of the execution was achievement to a specified error, on the basis of varying radius. Thus, this network could determine the radius that performs the results best. According to Table 5 the radius of 2.5 of RBF has the best performance to reproduce tidal data.

Figure 5 shows the distribution graph of the tidal condition derived from the three-layer FFBP network (Figure 5A), the RBF network (Figure 5B), and the harmonic analysis (Figure 5C) against the field data, for the year 2018. Accumulation of data around the diagonal axis (fit) indicates the proper performance of the three-layer FFBP network. It can be seen that the correlation coefficient is 0.85 for the three-layer FFBP neural network, 0.81 for the RBF network, and 0.83 for the harmonic analysis, which shows the acceptable accuracy of the three-layer FFBP neural network in predicting tidal condition, following by the RBF network.

Table 5: Test of various radius in the RBF network

Radius	Number of neurons	MSE
0.5	1650	1.830
1	300	0.536
1.5	50	0.153
2	50	0.129
2.5	***50***	***0.125***
3	0	0.129

Table 6: Correlation coefficient and MSE for predicting tidal condition in Beris port using FFBP network, RBF network, and harmonic analysis

Model	correlation coefficient	MSE
FFBP network	***0.85***	***0.101***
RBF network	0.81	0.125
Harmonic analysis	0.83	0.123

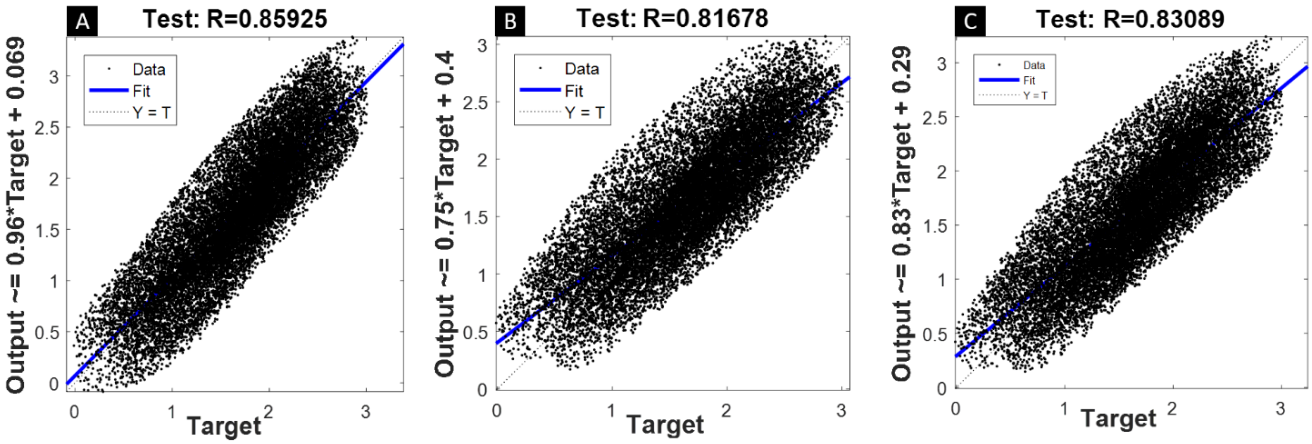

Figure 5: Distribution graph for one year tidal condition prediction using; A) FFBP network, B) RBF network, and C) Harmonic analysis against field data

Figure 6 presents the time series of tidal conditions predicted using the three-layer FFBP network, RBF network, and Harmonic analysis method, in comparison with the field data for the first 1000 time steps of 2018, (from 2018/01/01 to 2018/21/01). According to the figure, the tidal condition predicted by the FFBP network is in the best agreement with the field data.

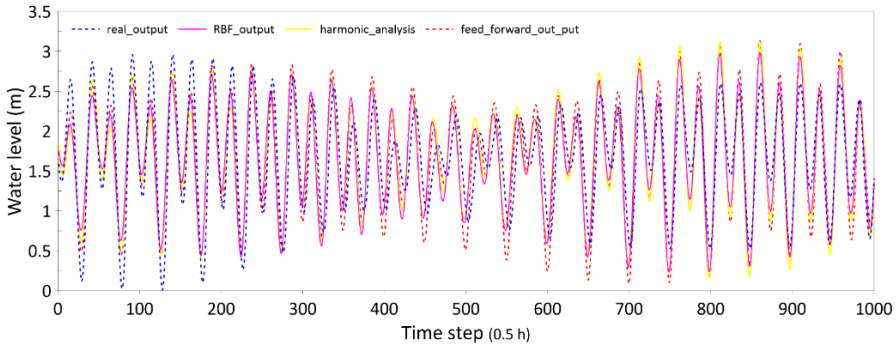

Figure 6: Time series of tidal condition predicted using FFBP network, RBF network, and Harmonic Analysis, in compare with the field data at Beris port for the year 2018 (from 2018/01/01 to 2018/21/01)

4. Conclusions

Even though the tidal water level is relatively easy to predict, its precision however depends on the number of tidal constituents that are considered for the prediction. In this research, the artificial neural network has been applied for this purpose. A feed forward back propagation neural network without hidden layer has been employed to provide the most relevant tidal constituents and their representative amplitude for Bris port, located in the northern of Gulf of Oman. According to the outcome M_2, K_1, S_2, N_2 and O_1 are the five major constituents, with the respective amplitudes of 0.44, 0.2, 0.19, 0.14, and 0.11, which play main role in the area. These five tidal constituents have been used for the prediction of tidal conditions for the year 2018 at Beris port. For this progress, two different neural networks were considered, including feed-forward backpropagation and radial bias function. The results then were compared with the harmonic analysis results and field data. It was found that the three-layer feed-forward backpropagation network with 60 days of training and 5 neurons in the hidden layer gives the best performance in terms of MSE error (0.101), correlation coefficient (0.85), and time consumption. For the radial bias function network the best performance was achieved with the radial 2.5, with the correlation coefficient of 0.81.

References

[1] *W. Wang and H. Yuan, "A Tidal Level Prediction Approach Based on BP Neural Network and Cubic B-Spline Curve with Knot Insertion Algorithm," Mathematical Problems in Engineering, vol. 2018, 2018.*

[2] *D. Pugh and P. Woodworth, Sea-level science: understanding tides, surges, tsunamis and mean sea-level changes. Cambridge University Press, 2014.*

[3] *M. Guan et al., "A method of establishing an instantaneous water level model for tide correction," Ocean Engineering, vol. 171, pp. 324–331, 2019.*

[4] *S. Cai, L. Liu, and G. Wang, "Short-term tidal level prediction using normal time-frequency transform," Ocean Engineering, vol. 156, pp. 489–499, 2018.*

[5] *G. W. Platzman, "Ocean tides and related waves," Mathematical problems in the geophysical sciences, vol. 14, no. Part 2, pp. 239–291, 1971.*

[6] *B. Hong et al., "Potential physical impacts of sea-level rise on the Pearl River Estuary, China," Journal of Marine Systems, vol. 201, p. 103245, 2020.*

[7] *Y. H. Song, Q. X. Xuan, and A. T. Johns, "Comparison studies of five neural network based fault classifiers for complex transmission lines," Electric power systems research, vol. 43, no. 2, pp. 125–132, 1997.*

[8] *B. B. Parker, "Tidal analysis and prediction.," 2007.*

[9] *E. A. Fanjul, B. P. Gómez, and I. R. Sánchez-Arévalo, "A description of the tides in the Eastern North Atlantic," Progress in Oceanography, vol. 40, no. 1, pp. 217–244, 1997.*

[10] *T.-L. Lee, "Back-propagation neural network for long-term tidal predictions," Ocean Engineering, vol. 31, no. 2, pp. 225–238, 2004.*

[11] *T.-L. Lee, O. Makarynskyy, and C.-C. Shao, "A combined harmonic analysis--artificial neural network methodology for tidal predictions," Journal of Coastal Research, vol. 23, no. 3 (233), pp. 764–770, 2007.*

[12] *O. Okwuashi and D. N. Olayinka, "Tide modelling using the Kalman filter," Journal of Spatial Science, vol. 62, no. 2, pp. 353–365, 2017.*

[13] *O. Okwuashi, C. Ndehedehe, and H. Attai, "Tide modeling using partial least squares regression," Ocean Dynamics, vol. 70, no. 8, pp. 1089–1101, 2020.*

[14] *G. Li, Y. Hao, and Y. Zhao, "Research of neural network to tidal prediction," in 2009 International Joint Conference on Computational Sciences and Optimization, 2009, vol. 2, pp. 282–284.*

[15] *F. A. Madah, "The amplitudes and phases of tidal constituents from Harmonic Analysis at two stations in the Gulf of Aden," Earth Systems and Environment, vol. 4, no. 2, pp. 321–328,*

2020.

[16] R. O. Strobl and F. Forte, "Artificial neural network exploration of the influential factors in drainage network derivation," Hydrological Processes: An International Journal, vol. 21, no. 22, pp. 2965–2978, 2007.

[17] R. Özçelik, M. J. Diamantopoulou, J. R. Brooks, and H. V Wiant Jr, "Estimating tree bole volume using artificial neural network models for four species in Turkey," Journal of environmental management, vol. 91, no. 3, pp. 742–753, 2010.

[18] J. A. Anderson, An introduction to neural networks. MIT press, 1995.

[19] A. M. Salim, G. S. Dwarakish, K. V Liju, J. Thomas, G. Devi, and R. Rajeesh, "Weekly prediction of tides using neural networks," Procedia Engineering, vol. 116, no. 1, pp. 678–682, 2015.

[20] B. L. Meena and J. D. Agrawal, "Tidal level forecasting using ANN," Procedia Engineering, vol. 116, pp. 607–614, 2015.

[21] L. Pashova and S. Popova, "Daily sea level forecast at tide gauge Burgas, Bulgaria using artificial neural networks," Journal of Sea Research, vol. 66, no. 2, pp. 154–161, 2011.

[22] M. Janati, M. Kolahdoozan, and H. Imanian, "Artificial Neural Network Modeling for the Management of Oil Slick Transport in the Marine Environments," Pollution, vol. 6, no. 2, pp. 399–415, 2020.

[23] S.-W. Kim, A. Lee, and J. Mun, "A Surrogate Modeling for Storm Surge Prediction Using an Artificial Neural Network," Journal of Coastal Research, no. 85, pp. 866–870, 2018.

[24] W. J. Palm, Introduction to MATLAB 7 for Engineers, vol. 7. McGraw-Hill New York, 2005.

[25] A. J. Adeloye and A. De Munari, "Artificial neural network based generalized storage--yield--reliability models using the Levenberg--Marquardt algorithm," Journal of Hydrology, vol. 326, no. 1–4, pp. 215–230, 2006.

[26] M. T. Hagan and M. B. Menhaj, "Training feedforward networks with the Marquardt algorithm," IEEE transactions on Neural Networks, vol. 5, no. 6, pp. 989–993, 1994.

[27] R. Battiti, "First-and second-order methods for learning: between steepest descent and Newton's method," Neural computation, vol. 4, no. 2, pp. 141–166, 1992.

[28] Z.-G. Zhang, J.-C. Yin, and C. Liu, "A modular real-time tidal prediction model based on Grey-GMDH neural network," Applied Artificial Intelligence, vol. 32, no. 2, pp. 165–185, 2018.

[29] M. H. Beale, M. T. Hagan, and H. B. Demuth, "Neural Network Toolbox™, User's Guide, MATLAB®R2015a, The MathWorks," Inc., Natick, MA, USA, vol. 410, 2015.

[30] S. E. Vt and Y. C. Shin, "Radial basis function neural network for approximation and estimation of nonlinear stochastic dynamic systems," IEEE transactions on neural networks, vol. 5, no. 4, pp. 594–603, 1994.

[31] J. Yin, Z. Zou, and F. Xu, "Sequential learning radial basis function network for real-time tidal level predictions," Ocean engineering, vol. 57, pp. 49–55, 2013.

[32] S. Ardani and M. Soltanpour, "Modelling of sediment transport in Beris fishery port," Civil Engineering Infrastructures Journal, vol. 48, no. 1, pp. 69–82, 2015.

[33] D. Ghaderi and M. Rahbani, "Detecting shoreline change employing remote sensing images (Case study: Beris Port-east of Chabahar, Iran)," International Journal of Coastal and Offshore Engineering, vol. 3, pp. 1–8, 2020.

[34] M. Sayehbani and D. Ghaderi, "Numerical Modeling of Wave and Current Patterns of Beris Port in East of Chabahar-Iran," International Journal of Coastal and Offshore Engineering, vol. 3, no. 1, pp. 21–29, 2019.

[35] C. Amante and B. W. Eakins, "ETOPO1 arc-minute global relief model: procedures, data sources and analysis," 2009.

[36] United States Geological Survey, "EarthExplorer," 2020. https://earthexplorer.usgs.gov/ (accessed Aug. 02, 2020).

[37] A. Zhang, J. Yin, J. Hu, and C. Yu, "Modular tidal level short-term forecasting based on BP neural networks," in Proceedings of the 33rd Chinese Control Conference, 2014, pp. 5037–5042.

[38] M. G. Foreman, "G, 1977: Manual for tidal heights analysis and prediction," Pac. Mar. Sci. Rep, vol. 77, no. 10, 1977.

[39] G. Dietrich and K. Kalle, "General oceanography; an introduction," 1957.

[40] M. Mahmoudof and M. Bagheri, "Determination of Compound and Overtide Constituents near the Eastern Iranian Coast of Makran," Journal of Oceanography, vol. 10, no. 37, pp. 33–41, 2019, doi: 10.29252/joc.2019.10.12162.

[41] K. Hornik, M. Stinchcombe, H. White, and others, "*Multilayer feedforward networks are universal approximators*.," Neural networks, vol. 2, no. 5, pp. 359–366, 1989.

[42] E. Sertel, H. K. Cigizoglu, and D. U. Sanli, "*Estimating daily mean sea level heights using artificial neural networks*," Journal of Coastal Research, vol. 24, no. 3 (243), pp. 727–734, 2008.